Gu et al.
Journal of Engineering and Applied Science (2024) 71:39
https://doi.org/10.1186/s44147-024-00369-y

Journal of Engineering and Applied Science

RESEARCH **Open Access**

Bearing capacity prediction of the concrete pile using tunned ANFIS system

Wei Gu[1], Jifei Liao[2] and Siyuan Cheng[1*]

*Correspondence: cheng_siyuan1226@163.com

[1] Sichuan University Jinjiang College, Meishan 620860, Sichuan, China
[2] China Mcc5 Group Corp. Ltd, Chengdu 610000, Sichuan, China

Abstract

The design process for pile foundations necessitates meticulous deliberation of the calculation pertaining to the bearing capacity of the piles. The primary objective of this work was to investigate the potential use of Coot bird optimization (CBO) techniques in predicting the load-bearing capacity of concrete-driven piles. Despite the availability of several suggested models, the investigation of Coot bird optimization (CBO) for estimating the pile-carrying capacity has been somewhat neglected in this research. This work presents and validates a unique approach that combines the Coot bird optimization (CBO) model with the Multi-layered perceptron (MLP) neural network and adaptive neuro-fuzzy inference system (ANFIS). The findings of 472 different driven pile static load tests were put in a database. The proposed framework's building, validation, and testing stages were each accomplished utilizing the training set (70%), validation set (15%), and testing set (15%) of the dataset, respectively. According to the findings, MLP_{CBO} and $ANFIS_{CBO}$ both offer remarkable possibilities for accurately predicting the pile-bearing capacity of a given structure. The R^2 values for $ANFIS_{CBO}$ during the training stage were 0.9874, while during the validating stage, they were 0.9785, and during the testing stage they were 0.987. After considering various kinds of performance studies and contrasting them with existing literature, it has been concluded that the $ANFIS_{CBO}$ model provides a more appropriate calculation of the bearing capacity of concrete-driven piles.

Keywords: Bearing capacity, Concrete piles, ANN, ANFIS, Coot optimization algorithm

Introduction

To sustain superstructures with enormous loads or those situated on unstable ground, deep foundations are a typical and essential form of foundation [1]. Driven piles composed of wood, steel, precast concrete, and composite are another cost- and quality-efficient alternative to drilled shafts. The axial pile-bearing capability is considered the most significant factor when designing a pile foundation. As a result, many theoretical and empirical geotechnical research has focused on calculating this value.

The pile-bearing capability may be assessed using five primary techniques: static analysis, dynamic analysis, dynamic testing, pile load test, and in-situ testing [2–5]. It is often suggested to use the essential depth idea in design recommendations according to static analysis. The crucial depth, nevertheless, is an idealization that defies physical principles and lacks theoretical or trustworthy empirical evidence.

The hammer-pile-soil system is subject to dynamic analysis using wave mechanics as a foundation. Uncertainties in calculating bearing capability are brought on by the hammer impact effect's ambiguity and also by variations in soil power due to environmental factors at the time of pile drive and loading. The measurement of velocity and force close to the pile head during driving is the foundation of dynamic testing techniques. Nevertheless, a skilled individual is able to interpret the evaluations. The capability estimate is also not known until the pile is driven, which is a significant restriction [6]. The full-scale pile settlement under a static load is measured in the field in a pile load test, which is thought to convey the most precise findings. This approach, nevertheless takes a lot of time and money [7]. So, it is crucial to create a straightforward, cost-effective, and precise procedure.

Since the 1970s, in situ test techniques for measuring soil parameters have progressed quickly. This advancement is being accompanied by an increase in the estimation of pile-bearing capability using data from in-situ tests. Standard penetration test (SPT), cone penetration test (CPT), flat dilatometer test (DMT), pressuremeter test (PMT), plate loading test (PLT), dynamic probing test (DP), press-in and screw-on probe test (SS), and field vane test (FVT) are a few examples of typical tests. In an effort to assess the material properties, every test employs several loading techniques to quantify the related soil reaction. The SPT is often utilized to forecast the piles' bearing capability between these in-situ test data [8, 9].

In the research, many SPT data-based approaches for calculating pile-bearing capacities have been developed. Direct and indirect techniques are the two categories into which they fall. Because of their simplicity in calculation, the direct techniques are preferred by field engineers. For instance, SPT direct approaches for sandy or clayed soil were presented in [10–15]. The researchers used the limited component approach to assess the pile for a case investigation in Iran [15] and contrasted the results with four distinct SPT direct techniques to arrive at an accurate forecast of the pile's bearing capability. Nevertheless, every one of these experimental formulations have certain shortcomings, based on [4]. As a result, scholars have started searching for various techniques to forecast pile-bearing capability using SPT data. Utilizing machine learning techniques may be successful, according to earlier research [16].

Machine learning (ML), a subset of artificial intelligence that simulates the human brain's functioning, is capable of inferring novel information nonlinearly from past data via adaptive learning [17–24]. Additionally, as learning data increases, the machine learning (ML)-based models' efficiency may be enhanced progressively, keeping them current with the strict precision demands for complicated engineering challenges [25–30]. Numerous studies have shown how well ML-based models work in solving issues associated to civil engineering, such as forecasting the mechanical characteristics (compressive/tensile strength/shear) of hardened concrete [31–34], the ultimate bond strength of corroded reinforcement and surrounding concrete [35, 36], the bearing capability of piles [37, 38], the pulling capability of ground anchors [39–41], and others.

Artificial neural networks (ANN), in particular, have been widely employed in ML-based models to forecast pile-bearing capability. Previous attempts in this manner may be seen in [42, 43], which use ANN with error back propagation. Utilizing results from 50 dynamic load tests performed on prefabricated concrete piles, [44] combines ANN with genetic algorithm (GA), with the weights of ANN being adjusted by GA. Identical methods are suggested in [45], where the ANN connection weights are optimized using particle swarm optimization (PSO) along with GA. When using ANN to forecast the piles' bearing capability, GA is also utilized to identify the most crucial characteristics in the unprocessed dataset [3]. Other ML-based approaches than ANN have also been taken into account; for example, Samui [46] employs support vector machine (SVM), Pham et al. [2] explore random forest, and Chen et al. [38] investigated the neuro-imperialism and neuro-genetic approaches.

Many studies employed a number of machine learning techniques to successfully measure the foundation's bearing capabilities. For the purpose of predicting the bearing capacity of the thin-walled foundation, ANN models were developed utilizing a total of 150 specimens, and an adaptive neuro-fuzzy inference system (ANFIS) was developed as well [47]. The researchers obtained the coefficient of determination (R^2) and root mean squared error (RMSE) values for the ANFIS and ANN models, which were determined to be 0.875 and 0.048, and 0.71 and 0.529, accordingly. In an alternative study, the determination of pile bearing capability included the use of 296 sets of data and the application of Gaussian process regression analysis, resulting in an R^2 value of 0.84 [48]. In their study, Kulkarni et al. [49] used a dataset consisting of 132 data points to elucidate the behavior of rock-socketed piles. This was achieved by using a hybrid approach that combined the genetic algorithm (*GA*) technique with artificial neural networks (ANN). The researchers obtained a coefficient of determination (R^2) value of 0.86 and a root mean square error (RMSE) value of 0.0093. Using this dataset and a hybrid model known as particle swarm optimization (PSO)-ANN, another group of researchers were able to replicate the behavior of rock-socketed piles [50]. Their results showed an R^2 value of 0.918 and an RMSE value of 0.063. The dataset used in previous empirical endeavors to construct models consisted of a total of 472 specimens [3, 51]. Models that were taken into account included a hybrid deep neural network (DNN) with genetic algorithm (GA), as well as a hybrid whale optimization (WOA) technique with extreme gradient boosting (XGB). The R^2 and RMSE values that were generated by the GA-DNN model came out to be 0.882 and 109.965, accordingly. The findings for WOA-XGB showed significant improvement, with R^2, and RMSE values of 0.97 and 64 during the training step, and 0.94 and 87.03 at the testing step, respectively.

In conclusion, the present study has made some notable contributions, which may be outlined as follows:

- In this study, a comprehensive dataset including 472 pile test findings is used to develop and validate machine learning models for the assessment of pile-bearing capacity. It is essential to acknowledge that prior research has often concentrated on limited datasets.
- The investigation of coot bird optimization (CBO) for assessing the load-bearing capacity of piles has been somewhat neglected in scholarly research, despite the existence of numerous suggested models.
- The selection of the appropriate model, which entails the selection of the appropriate hyper-parameters, is of the utmost importance. This work presents and validates a unique approach that combines the coot bird optimization (CBO) model the multi-layered perceptron (MLP) neural network and the adaptive neuro-fuzzy inference system (ANFIS).

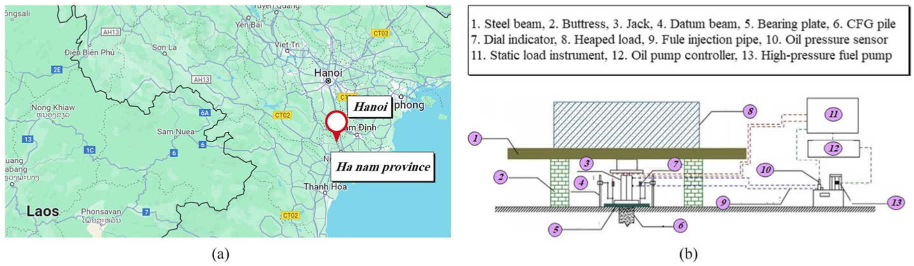

Fig. 1 **a** Experimental position. **b** Static load test experiment to record bearing capacity of pile [3]

Methods

Data description and pre-processing

The dataset used for training and evaluating the machine learning approach described in this paper consists of findings of static load tests conducted on driven strengthened concrete piles. The 472 pieces of data that are now included in this collection were obtained for previous research [3]. The adequacy of the data collection for the development and validation of advanced machine-learning models is attributed to its substantial size. In order to evaluate the capacity of the precast piles, hydraulic pile-driving machinery is used to drive the piles into the soil layers. The piles have closed tops. Figure 1 illustrates the testing environment, including the data gathering apparatus, as well as the specific testing site. The bearing capacity of piles was determined using a static load test experiment detailed in Fig. 1b. Figure 2 is a graphic representation of the pile structure, which includes the geometrical factors associated with it as well as the location of the soil layers. The following are categories of input parameters: In_1) pile's diameter (mm), In_2) the first soil layer's thickness that piles embedded (m), In_3) the second soil layer's thickness that pile embedded (m), In_4) the third soil layer's thickness that piles embedded (m), In_5) top elevation of pile (m), In_6) natural ground elevation (m), In_7) the extra segment pile top's elevation (m), In_8) the pile tip's depth (m), In_9) the mean SPT blow count along the pile shaft, and In_{10}) the mean SPT blow count at the pile tip [3]. Table 1 contains an overview of all ten of the conditioning variables that were considered while making a prediction about the dependent parameter (axial pile bearing capacity). These variables are denoted by the notation In_1 through In_{10}. Along with other pieces of information, this table also provides a statistical analysis of the independent parameters as well as the parameters that are being predicted. The dataset contains 472 pieces of data, and it was partitioned into three distinct subsets: the testing set, which comprises 15% of the dataset (or 71 data), the validation set, which also comprises 15% of the dataset (or 71 data), and the training set, which comprises 70% of the dataset (or 330 data) [3, 51]. The data points are extracted from the bigger database via a standard diffusion and are then picked at random. An investigation using statistics was performed so that the practicability of the input parameters could be evaluated. Additionally, the input and outcome factor distribution diagrams are shown in Fig. 3.

The degree to which the data points in a scatterplot conform to a linear pattern is measured by the Pearson correlation coefficient [52], which provides a numerical value. The primary objective of the Pearson correlation coefficient is to ascertain the degree of association between two variables. The range of the coefficient is from -1 to $+1$. A positive numerical value indicates a positive linear relationship, whereby there is a propensity for

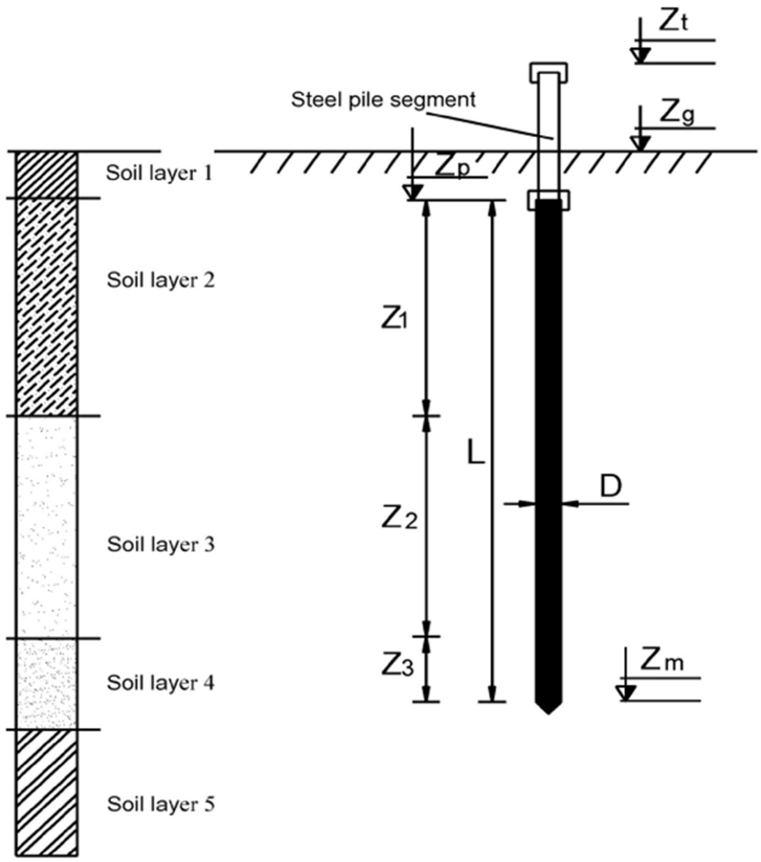

Fig. 2 Plot for stratigraphy and pile variables [3]

both parameters to increase together. A negative number indicates a negative linear relationship, whereby there is a tendency for the other variable to decrease as one parameter increases. Values closer to + 1 or − 1 indicate a powerful linear relationship, while values closer to 0 suggest a weak or negligible linear correlation. The Pearson correlation coefficient is shown here in Fig. 4. The study may have been not capable of effectively capturing the impact of substantial negative or positive Pearson correlation coefficient variables on the findings due to a potential deficiency in powerful technique. It is noteworthy to observe that there are not many deviations from the high association values that exist among the parameters. As a consequence of this, the development of models that make use of these inputs needs to be successful for the purpose of reaching the highest possible accuracy. It is evident that a significant proportion of the association values exhibit high magnitudes. Among the investigated variables, the highest positive value is seen for In_8 and In_3, both having a value of 0.99. The most negative value is seen in In_5 and In_2, measuring -0.96.

Applied optimizer and frameworks

Coot bird optimization (CBO)

The COOT method, developed by Iraj Naruei et al. (2021), is a recently introduced meta-heuristic optimization technique that aims to replicate the collective behavior of a swarm of coot birds. In comparison to other optimization methods, including the particle swarm optimization method and the differential evolution method, the COOT

Table 1 Statistical description of the input and output variables

Phase	Metric					
	Minimum	**Maximum**	**Standard deviation**	**Skewness**	**Kurtosis**	**Average**
Inputs						
Diameter of pile (*mm*) (In_1)						
Training	300	400	48.432	− 0.515	− 1.745	362.424
Validating	300	400	48.546	− 0.504	− 1.798	361.972
Testing	300	400	44.9823	− 0.9917	− 1.0468	371.831
The thickness of the first soil layer that pile embedded (*m*) (In_2)						
Training	3.4	5.72	0.491	0.642	− 0.730	3.821
Validating	3.4	4.45	0.447	0.372	− 1.815	3.794
Testing	3.4	4.75	0.46495	0.1379	− 1.756	3.87746
The thickness of the second soil layer that pile embedded (*m*) (In_3)						
Training	1.5	8	1.574	− 0.946	0.517	6.594
Validating	1.71	8	1.700	− 1.029	0.638	6.532
Testing	1.66	8	1.83948	− 1.2861	0.92027	6.5569
The thickness of the third soil layer that pile embedded (*m*) (In_4)						
Training	0	1.69	0.450	0.893	− 0.984	0.321
Validating	0	1.13	0.446	0.856	− 1.167	0.326
Testing	0	1.22	0.48996	0.63525	− 1.5594	0.38338
Pile top elevation (*m*) (In_5)						
Training	0.68	3.4	0.619	− 0.393	− 1.388	2.812
Validating	1.95	3.4	0.609	− 0.362	− 1.700	2.825
Testing	1.95	3.4	0.60256	− 0.0936	− 1.802	2.74225
Natural ground elevation (*m*) (In_6)						
Training	3.04	4.12	0.080	1.310	13.141	3.495
Validating	3.26	3.67	0.078	− 0.203	1.031	3.490
Testing	3.21	3.72	0.07878	− 0.6016	3.06421	3.50169
The elevation of extra segment pile top (*m*) (In_7)						
Training	1.03	4.05	0.598	− 0.667	− 0.982	2.929
Validating	2	3.58	0.577	− 0.532	− 1.458	2.914
Testing	1.99	4.35	0.61997	− 0.2142	− 1.3344	2.87549
The depth of pile tip (*m*) (In_8)						
Training	8.3	16.09	1.733	− 0.693	− 0.014	13.547
Validating	8.51	15.53	1.848	− 0.798	0.143	13.478
Testing	8.46	15.62	2.02017	− 1.0291	0.34365	13.56
The average SPT blow count along the pile shaft (In_9)						
Training	5.6	15.41	2.220	− 0.156	− 1.234	10.746
Validating	5.81	13.49	2.291	− 0.203	− 1.192	10.653
Testing	5.76	13.57	2.41719	− 0.4566	− 0.9812	10.8177
The average SPT blow count at the pile tip (In_{10})						
Training	4.38	7.73	0.617	− 1.926	5.366	7.064
Validating	4.56	7.7	0.685	− 2.111	5.405	7.047
Testing	4.52	7.75	0.80459	− 1.9101	3.43106	7.02746
Output						
The axial bearing capacity load of pile (*kN*)						
Training	423.9	1551	354.039	-0.090	-1.686	987.007
Validating	407.2	1551	360.570	-0.028	-1.625	956.177
Testing	423.9	1551	337.617	-0.1526	-1.5152	999.186

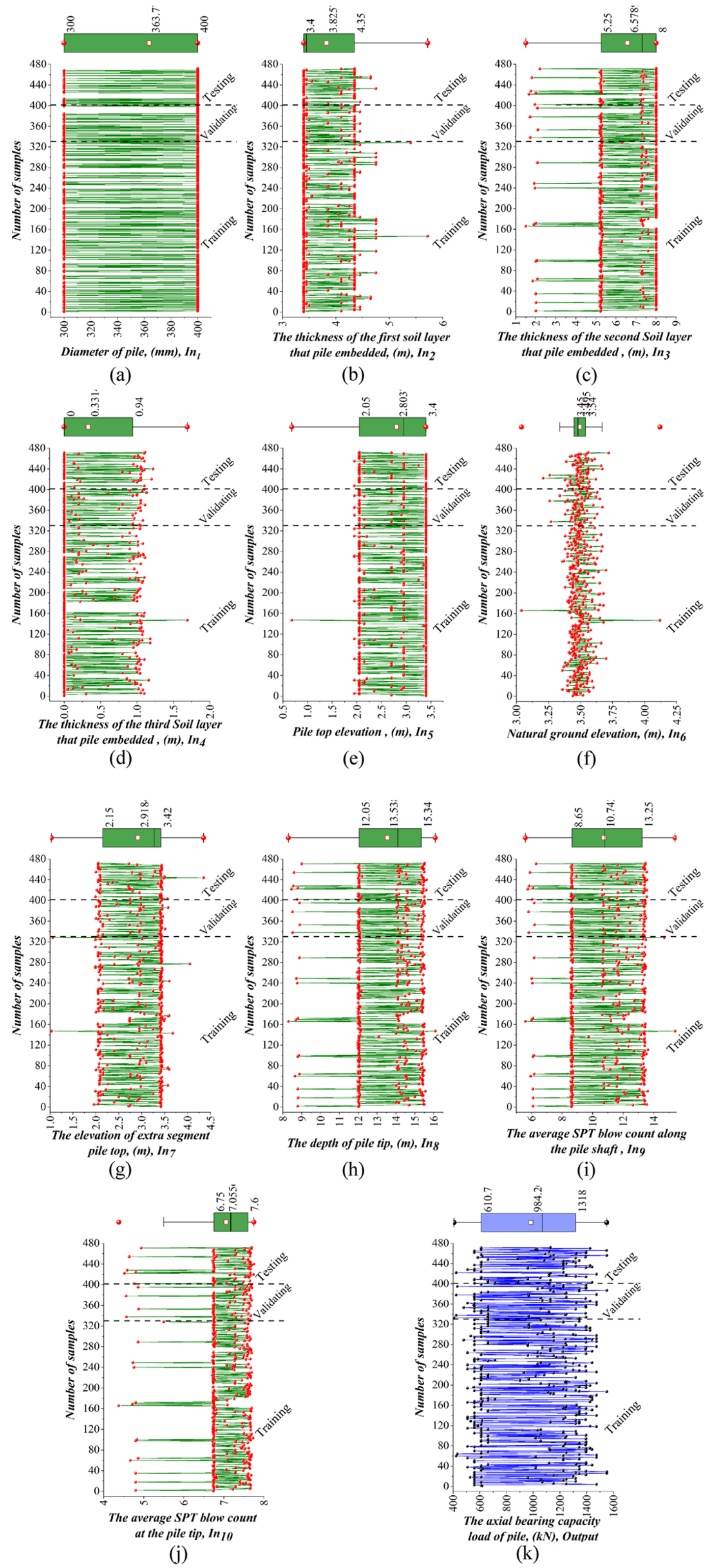

Fig. 3 Plot of input and output parameters. **a**–**j** Input variables. **k** Output

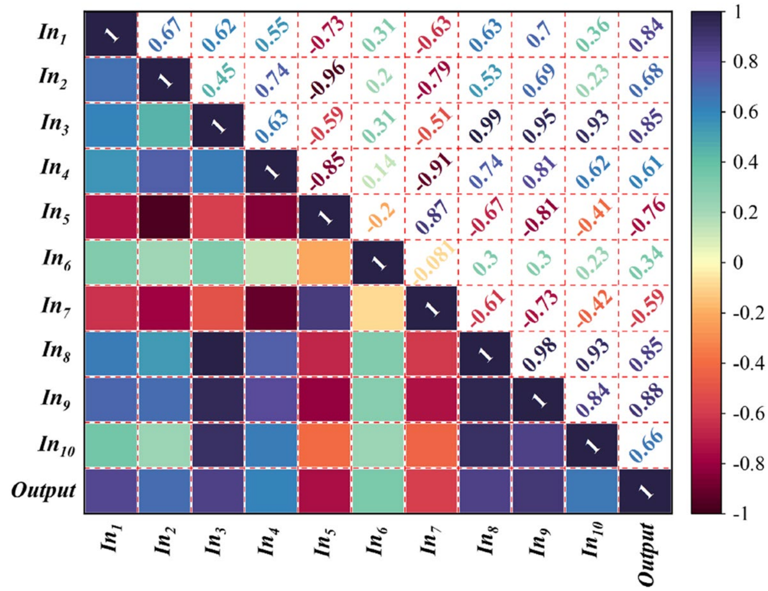

Fig. 4 PCC matrix

method has rapid convergence velocity and great precision in convergence. Furthermore, the COOT method has undergone validation in several engineering applications, including pressure vessel design, welded beam design, stepped cone pulley, and rolling bearing difficulties [53]. Hence, this study employs the COOT method as a solution to address the HDEED issue.

The underlying concept of the COOT method may be described below (Figs. 5 and 6).

(1) The first placement of the coot population will be established, followed by the computation of the associated fitness levels for each of these populations.

$$Q = Lb + \text{rand}(1, d) * (Ub - Lb) \tag{1}$$

The variable Q is formed by the process of randomly initializing people. The variable d reflects the dimension of the problem that has to be solved. Additionally, the variables Ub and Lb represent the highest and lowest bounds of the population positions. The matrix displaying the positions of the coot is shown below.

$$C\text{pos}^l = \left[x^l_{N,1}, x^l_{N,D}, \ldots, x^l_{N,D}\right] \tag{2}$$

Here, $C\text{pos}^l$ shows the entire coot position, and N shows the population's scale.

The inclusion of the coot's position is included in the fitness function, resulting in the generation of a fitness matrix for the coot population.

$$\text{Fit}^l = \left[fit^l_1, fit^l_2, \ldots, fit^l_N\right] \tag{3}$$

Here, fit^l_i shows the fitness value of the i_{th} individual at the time of the l_{th} iteration.

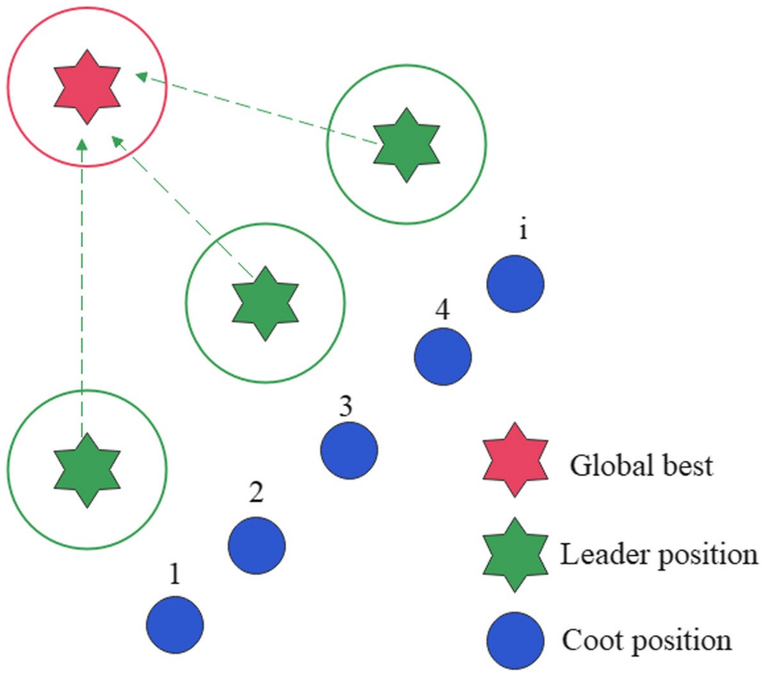

Fig. 5 Coots' leader selection mechanism [53]

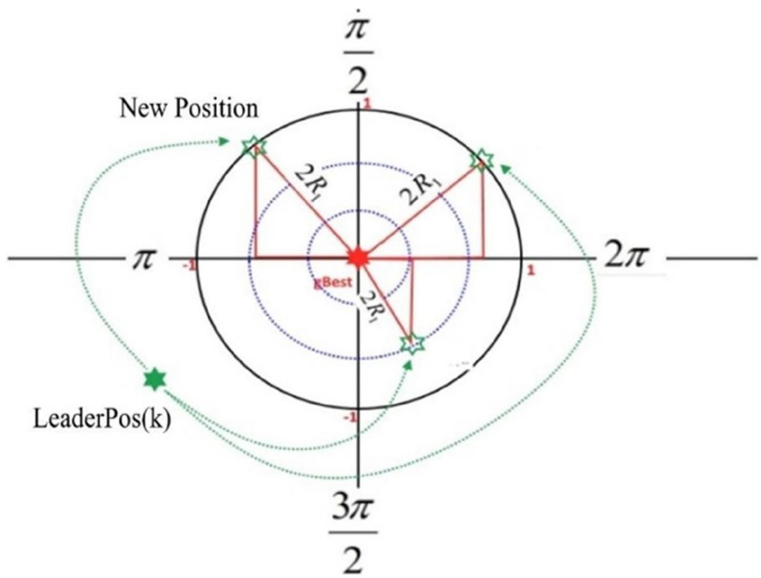

Fig. 6 Readjust the leaders' locations relative to the proper location [53]

(2) Common coot population position update

The current motion of the coot is modeled by simulating the collective motion of the population based on the distinct collective manners shown by the leader and the typical coot individual. Hence, there are four distinct patterns of movement seen on the water's surface, such as random movement, chain movement, movement guided by the leader of the general population, and optimum movement executed by the leader.

A location is generated at random inside the spatial domain, allowing a common one to afterward update the location. The formula governing the accidental mobility of the individual is as outlined below:

$$\mathrm{Cpos}(i) = \mathrm{C}pos(i) + A \times R2 \times (Q - \mathrm{Cpos}(i)) \tag{4}$$

Here, the location of the i_{th} the typical individual is denoted as $\mathrm{Cpos}(i)$, where A represents a decreasing integer ranging from 0 to 1, $R2$ indicates an accidental value between 0 and 1, and Q indicates an accidental location inside the search area. The following formula determines the values of A and Q in the following way:

$$\begin{cases} A = 1 - \frac{l}{L} \\ Q = rand(1, d) * (UB - LB) + LB \end{cases} \tag{5}$$

Here, l is the iterations' present number, and L is the iterations' highest number that may be performed, respectively.

A distance vector among two individuals updates the location throughout the typical population chain movement. The formula for the chain is outlined below:

$$\mathrm{Cpos}(i) = 0.5 \times (\mathrm{Cpos}(i-1) + \mathrm{Cpos}(i)) \tag{6}$$

In the context of leader-based location modification, the typical individual is required to modify its location by means of the k_{th} leader.

$$Cpos(i) = Lpos(k) + 2 \times R1 \times \cos(2R\pi) \times (Lpos(k) - Cpos(i)) \tag{7}$$

Where $Lpos(k)$ is the k_{th} leader's location, $R1$ represents an accidental integer within the range [0,1], and the variable k is selected in the manner outlined below:

$$k = 1 + (iMODm) \tag{8}$$

In this equation, m represents the total number of leaders, and i indicates the present member of the i_{th} coot group.

(3) Position update of the leader population

As part of the leader's location modification, it is not uncommon for the leader to abdicate the currently finest location in order to assist in the discovery of a location that is more advantageous. If a leader is looking for a finer location, the ideal location from the prior instant should be assigned to the leader; alternatively, the leader should return to the place they were in before. The following outlines the leader's location:

$$L\mathrm{pos}(i+1) = \begin{cases} B \times R3 \times \cos(2R\pi) \times \left(\mathrm{gbest} - \mathrm{Lpos}(i)\right) + gbestR4 < 0.5 \\ B \times R3 \times \cos(2R\pi) \times \left(\mathrm{gbest} - \mathrm{Lpos}(i)\right) - gbestR4 \geq 0.5 \end{cases} \tag{9}$$

The variables $R3$ and $R4$ denote accidental values within the range of 0 to 1, whereas $g$best indicates the present ideal position. The modified position of variable B is outlined below:

$$B = 2 - l/L \tag{10}$$

Multi-layered perceptron (MLP) neural network

According to [54], ANN models are strong non-linear modeling techniques that operate by mimicking the functioning of the human brain. They are computer models for information processing. When the input and outcome parameters are mapped into a complicated network, an ANN may assess nonlinear functions. This research utilized a popular ANN with one input level, one outcome level, and at minimum one concealed level that was first put out by [55]. According to [56], the ANN might be represented in the following way:

$$y_i = f\left(\sum_{i=1}^{N} w_{ji}x_i + b_i\right) \tag{11}$$

Here, x_i stands for the i_{th} nodal value, N for the nodes' number, in the prior level; f shows the j_{th} nodal value, y_i shows the j_{th} node's bias, b_i denotes the activation function, and w_{ji} stands for a weight-linking x_i and y_i.

Numerous investigations have shown that the ANN model can predict complicated nonlinear functions for hydrological data with only one concealed level [57]. According to our research's preliminary findings, the link between the groundwater level and the other hydrologic cycle elements may be roughly approximated by one concealed level. Although optimal practices for finding the volume of the concealed nodes have also been offered, calculating the volume of the concealed nodes is commonly carried out by examination and mistake and is a crucial component of the ANN. According to Huang's (2003) research, the following amount of concealed nodes is required to learn N^i samples with a little tiny fault:

$$N^H = 2\sqrt{(N^o + 2)N^i} \tag{12}$$

Here, N^H shows the concealed nodes' highest volume, and N^i and N^o show the input nodes and outcome nodes. In this work, the concealed nodes' size was changed from one to N^H, and the ideal size was determined via a process of examination and mistake. For training, the Levenberg–Marquardt (LM) method, one of ANN s' most effective methods, was employed [58]. The back-propagation method is applied to learn the biases and weights, and the CBO algorithm determines the optimal neuron numbers in each hidden layer (Fig. 7). In this study, the maximum number of each hidden layer is assumed to be 25. According to the literature, two hidden layers are considered for MLP structure to predict the bearing capacity of the concrete pile. MLPs often have hyperparameters (e.g., learning rate, number of layers) that impact their performance. CBO was employed to perform hyperparameter tuning, searching through the hyperparameter space to find the best configuration for the MLP. MLPs may suffer from overfitting, especially with complex architectures. Regularization techniques were optimized using optimization algorithms to find the right balance between model complexity and generalization.

Adaptive neuro-fuzzy inference system (ANFIS)

The basic model in the present work uses ANFIS as a machine learning method. The Takagi–Sugeno fuzzy system approach, which underpins ANFIS, was first suggested by Jang et al. in 1993 [59]. ANFIS is capable of using both fuzzy logic and neural networks in a single frame if one thinks of it as an integrated notion. The ANFIS method's proper structure is chosen based on the input data, membership level, and input and result membership functions. By

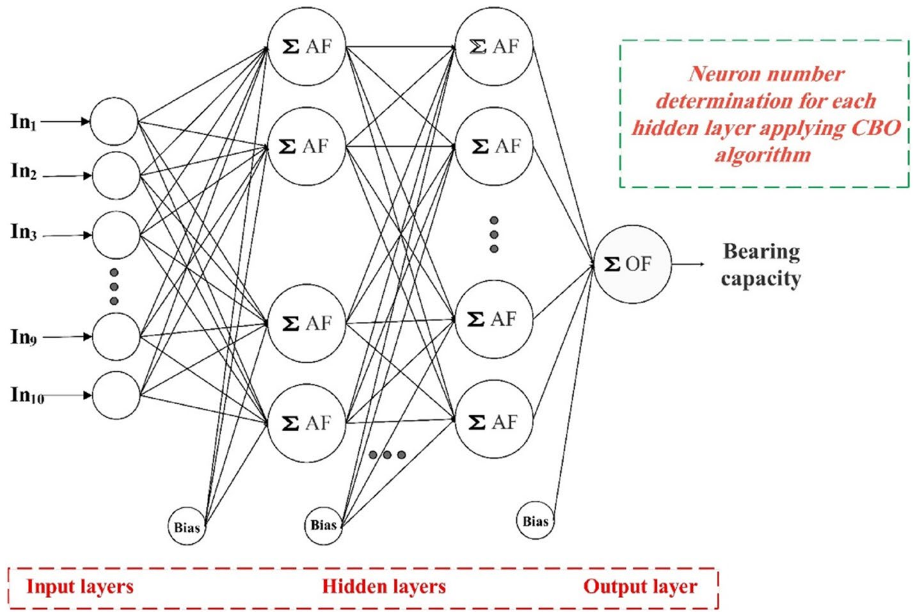

Fig. 7 The schematic of CBO − MLP

modifying the level of membership variables in accordance with the allowed rate of error throughout the training phase, input values are able to be closer to observed values. The ANFIS technique makes use of fuzzy logic and neural network learning methods to handle the nonlinear connection between the values of the input and the output. It has great potential for use in time series modeling and categorization problems [60]. Based on the benefits of fuzzy rules, numeric data may be collected from a technically written rule, and the ANFIS is able to easily assess the intricate conversion of mankind's intelligence into fuzzy systems. The fuzzy if–then principles that may be learned to estimate nonlinear functions are used in its inference mechanism. ANFIS is hence regarded as a well-liked estimating tool in engineering domains. ANFIS is hence regarded as a well-liked estimating tool in engineering domains. In this work, fuzzy grouping according to the k-means grouping method was done using the fuzzy cluster means (FCM) technique, and the optimal optimization technique for the traditional ANFIS was found using the backpropagation technique [61]. In the present work, the ANFIS model was implemented using fuzzy c-means (FCM) clustering by collecting the collection of rules required for producing the fuzzy inference system (FIS). Regarding ANFIS designs, a fundamental ANFIS design was created using the initial parameters. The CBO methodology was then used to optimize the developed ANFIS framework. The parameters of the membership function for the proposed system were enhanced by the use of the CBO method in this research. The RMSE index was calculated as a fitness indicator in order to assess the precision of the optimization framework. Finally, a hybridized and optimized $ANFIS_{CBO}$ network was defined, whereby the parameters of the network, such as the number of fuzzy words and the maximum number of iterations, were determined.

Indices to effectiveness evaluation

The performance comparison criteria were developed to fulfill the need for a standardized and quantifiable approach to assessing and comparing the overall efficiency of a number of different models. The use of these metrics enables the stakeholders to perform an evaluation of the performance of a number of answers, determine regions in need of development, and make choices based on accurate information. In this study, the following metrics were calculated and included in the analysis: coefficient of determination (R^2), root mean square error (RMSE), normalized root-mean-square (NRMSE), relative absolute error (RAE), root relative squared error (RRSE), and performance index (PI). Lower values of RMSE, RAE, RRSE, and PI are indicative of greater accuracy. Furthermore, a greater R^2 value signifies enhanced performance.

$$R^2 = \left(\frac{\sum_{d=1}^{D} (m_d - \overline{m})(z_d - \overline{z})}{\sqrt{\left[\sum_{d=1}^{D} (m_P - m)^2\right]\left[\sum_{d=1}^{D} (z_d - \overline{z})^2\right]}} \right)^2 \tag{13}$$

$$\text{RMSE} = \sqrt{\frac{1}{D}\sum_{d=1}^{D} (z_d - m_d)^2} \tag{14}$$

$$\text{NRMSE} = \text{RMSE}/\text{z}^{-} \tag{15}$$

$$\text{RAE} = \frac{\sum_{d=1}^{D} |m_d - z_d|}{\sum_{d=1}^{D} |m_d - \overline{m}|} \tag{16}$$

$$\text{RRSE} = \sqrt{\frac{\sum_{d=1}^{D} (m_d - z_d)^2}{\sum_{d=1}^{D} (m_d - \overline{m})^2}} \tag{17}$$

$$PI = \frac{1}{\overline{m}} \frac{RMSE}{\sqrt{R^2 + 1}} \tag{18}$$

In these equations, m_d, $\overline{m}$, z_d, and $\overline{z}$ are the observations, the average of the observations, the simulations, and the average of the simulations, respectively. Also, D depicts the total number of datasets.

Results and discussion

Model development

The determination of the bearing capacity of the concrete piles was conducted utilizing the hybridized CBO models as outlined in this study. The hybrid models denoted as MLP_{CBO} and $ANFIS_{CBO}$, were used to ascertain the maximum iterations and the count of fuzzy words via the employment of MLP and ANFIS techniques. The bearing capacity of the concrete piles was assessed and computed throughout the training, validation, and testing phases of the developed MLP_{CBO} and $ANFIS_{CBO}$ techniques, as seen in Fig. 8. The error distribution is shown on the right side of Fig. 8. The metrics R^2, RMSE, NRMSE, RAE, RRSE, and PI were used to conduct an analysis of how

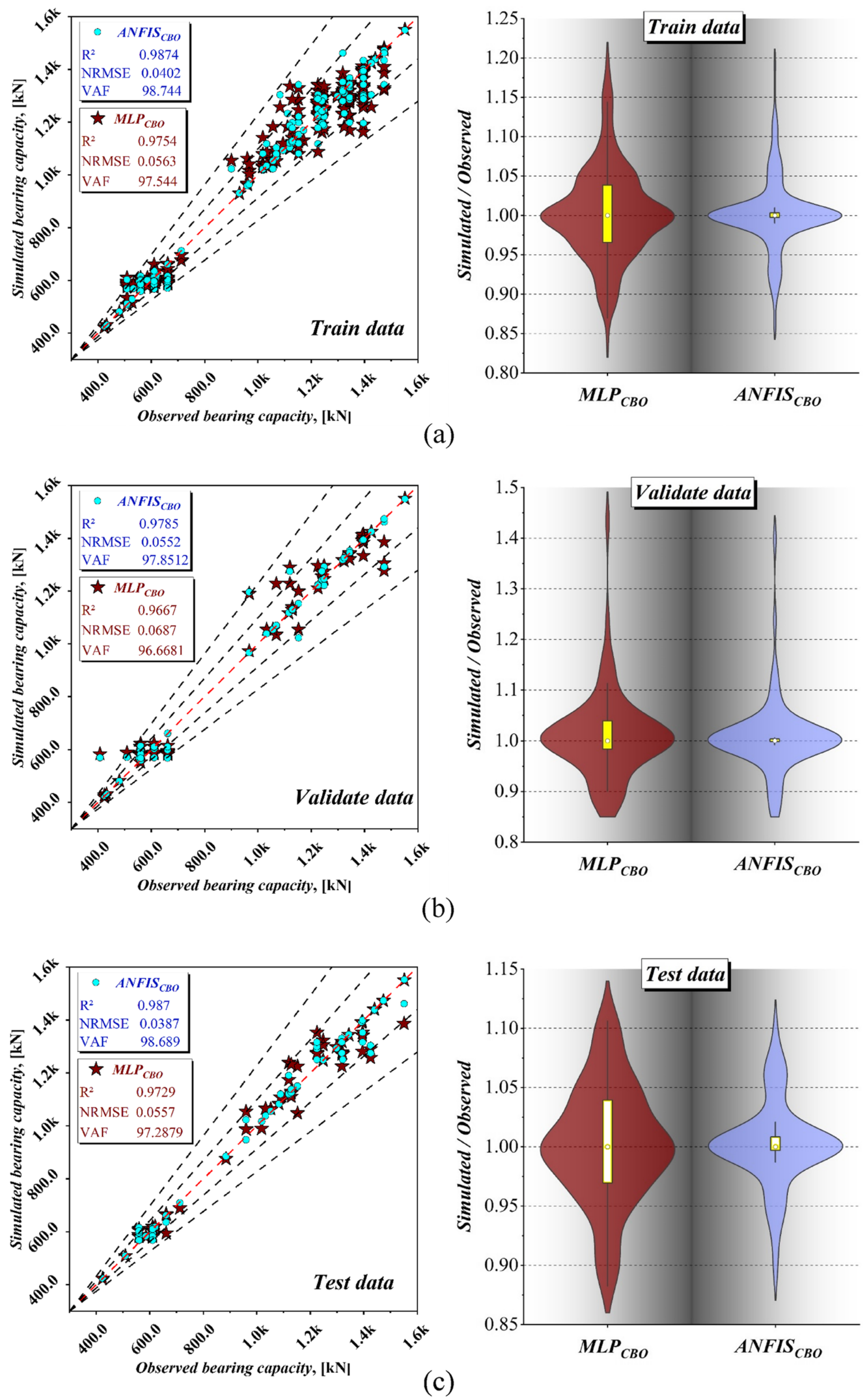

Fig. 8 The performance of the models. (right side: error, left side: correlation)

effective MLP_{CBO} and $ANFIS_{CBO}$ were in the research of procedure prediction (see Table 2 for more information). Furthermore, the reliability and efficacy of the developed models, namely XGB, WOA − XGB, and GA − DLNN, were assessed based on

Table 2 The *CBO*-based models' performance and literature comparison

Data	Index	Models		Literature		
		MLP_{CBO}	$ANFIS_{CBO}$	**XGB [51]**	**WOA-XGB [51]**	**GA-DLNN [3]**
Train data	R^2	0.9754	0.9874	0.99	0.97	0.944
	Score	1	2			
	RMSE	55.4829	39.6769	36.64	62.74	83.593
	Score	1	2			
	NRMSE	0.0563	0.0402			
	Score	1	2			
	RRSE	0.1567	0.1121			
	Score	1	2			
	VAF	97.5445	98.7441			
	Score	1	2			
Validate data	R^2	0.9667	0.9785			0.923
	Score	1	2			
	RMSE	65.9464	52.9064			95.118
	Score	1	2			
	NRMSE	0.0687	0.0552			
	Score	1	2			
	RRSE	0.1829	0.1467			
	Score	1	2			
	VAF	96.6681	97.8512			
	Score	1	2			
Test data	R^2	0.9729	0.987	0.92	0.94	0.887
	Score	1	2			
	RMSE	55.607	38.6543	101.3	87.72	110.17
	Score	1	2			
	NRMSE	0.0557	0.0387			
	Score	1	2			
	RRSE	0.1647	0.1145			
	Score	1	2			
	VAF	97.2879	98.6893			
	Score	1	2			
Summated score		15	30			

the results obtained from the present study, which primarily centered on the performance of these models. The findings were compared to those that were found in the previous research [3] and [51].

Based on the data, it seems that both the MLP_{CBO} and $ANFIS_{CBO}$ models have substantial potential for accurately predicting the pile-bearing capacity. During the training stage, the R^2 values for MLP_{CBO} were determined to be 0.954, while during the validating stage, they were 0.9667, and during the testing stage they were 0.9729. in a similar manner, the R^2 values for $ANFIS_{CBO}$ during the training, stage were 0.9874, while during the validating stage, they were 0.9785, and during the testing stage they were 0.987. Evaluating the dependability of a model based just on one metric is inadequate. In order to achieve this objective, it is important to conduct a comprehensive examination of a range of measures, including but not limited to RSME, NRMSE, RAE, RRSE, and PI. When one compares the percentages that are reported for MLP_{CBO} and $ANFIS_{CBO}$ for a variety of metrics, it is easy to see that $ANFIS_{CBO}$ reports a significant drop in comparison to MLP_{CBO}. The observed drop in performance demonstrates the high level of accuracy shown by the $ANFIS_{CBO}$ in estimating the bearing capacity of concrete piles.

In order to assess the reliability of the models, a comprehensive evaluation is conducted by comparing them with existing literature, specifically considering the models XGB [51, 51] WOA − XGB, and GA − DLNN [3]. A comprehensive examination of Table 2 reveals that the $ANFIS_{CBO}$ model, as introduced in this study, had favorable results in comparison to previous investigations discussed in the existing literature. The assessment was conducted using consistent metrics for the training, validation, and testing datasets, namely R^2 (coefficient of determination) and RMSE (root mean square error). The best model, $ANFIS_{CBO}$, has higher R^2 values and lower RMSE compared to XGB [51, 51]WOA − XGB, and GA − DLNN [3], indicating more precision and strength in its conclusions. For example, according to the results obtained from the WOA − XGB model, the coefficient of determination (R^2) increases from 0.97 to 0.9874 in the training stage and from 0.94 to 0.987 in the testing stage. Additionally, the metrics based on *RMSE* error shown a drop from 62.74 to 39.6769 in the training stage and from 87.72 to 38.6543 in the testing stage. A comprehensive comparison between $ANFIS_{CBO}$ and GA − DLNN [3] may be undertaken, taking into account the improvements seen in the training, validating, and testing data sets. These improvements include an increase in the values of R^2 and a decrease in the values of RMSE.

The distribution of the predicted/observed ratio of the algorithms throughout both the training and testing phases can be viewed on the right side of Fig. 8. Demonstrating enhanced efficacy is shown by a limited margin of error, including both a minimum and maximum threshold. The findings indicate that $ANFIS_{CBO}$ has higher efficacy in two phases, as shown by a decrease in error variability.

Recommendations for future studies

The focus of the current study was on the installation of driven reinforced concrete piles and their interaction with certain soil conditions. In the next research, it may be investigated how effectively the previously constructed machine learning models function with various soil profiles and pile kinds, such as drilled heaps and wood piles. Investigating ensemble models (such as random forests, gradient boosting, or model stacking techniques) might potentially enhance prediction accuracy even more. This is accomplished by combining a large number of machine-learning models. In subsequent research, field validation on actual construction projects may play a role, with the purpose of determining how useful the suggested models are when applied to actual-life circumstances. There is also the possibility of doing research on the challenges and considerations that go into effective implementation. It is feasible that by performing case studies on a variety of construction projects and contrasting the findings to the standards of the industry, it will be possible to learn a great deal about the effectiveness of machine learning models as well as the potential cost savings they may provide.

Sensitivity analysis

Sensitivity analysis is a technique used in various fields, including finance, engineering, environmental science, and decision-making processes [18]. The primary aim of sensitivity analysis is to assess how changes in the input parameters or assumptions of a model affect the output or outcomes. It helps in understanding the robustness and reliability of a model or system under different scenarios. Sensitivity analysis helps in identifying which variables or parameters have a significant impact on the model's output. By understanding the sensitivity of the model to different inputs, decision-makers can focus on key factors that drive the results. In the present, the procedure mentioned by Khatti, and Grover was chosen as a sensitivity analysis (S_a)'s method [62]. The results of the S_a was provided in Fig. 9. As it is clear from this plot, most of the input variables have high impact on the target higher than 0.9444, with some exceptions. The highest value belonged to *In*3 at 0.9836, while the lowest value was for In4 at 0.7216 of S_a (Table 3 in Appendix).

Conclusions

The hybridized CBO systems that were given in this study were used in order to evaluate the bearing capacity of the concrete piles. The hybrid models denoted as MLP_{CBO} and $ANFIS_{CBO}$, in which the MLP and ANFIS techniques were specified for the purpose of model augmentation. Furthermore, the reliability and robustness of the developed models, namely XGB, WOA − XGB, and GA − DLNN, were assessed based on the results obtained from the present study, which mostly centered on the produced models. The results obtained in this study were compared with the findings reported in previous research studies [3, 51].

1. Based on the data, it seems that both the MLP_{CBO} and the $ANFIS_{CBO}$ models have a great lot of potential for accurately forecasting the pile-bearing capacity. During the training stage, the R^2 values for MLP_{CBO} were determined to be 0.954, while during

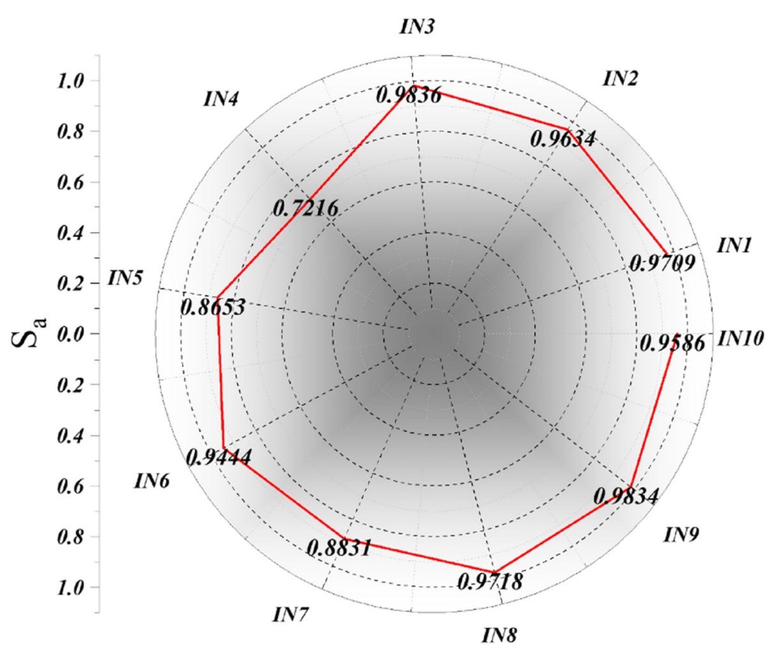

Fig. 9 The sensitivity analysis of variables on target

the validating stage, they were 0.9667, and during the testing stage they were 0.9729. In a similar manner, the R^2 values for $ANFIS_{CBO}$ during the training stage were 0.9874, while during the validating stage, they were 0.9785, and during the testing stage they were 0.987.

2. The comparison of the percentages of MLP_{CBO} and $ANFIS_{CBO}$ across several error-based measurements reveals a notable decrease in $ANFIS_{CBO}$ in comparison to MLP_{CBO}. The observed drop in performance demonstrates the high level of accuracy shown by the adaptive neuro-fuzzy inference system with coot bird optimization ($ANFIS_{CBO}$) in estimating the bearing capacity of concrete piles.
3. The results obtained from the $ANFIS_{CBO}$ model provides higher values of R^2 and lower RMSE compared to the XGB [51, 51]$WOA - XGB$, and $GA - DLNN$ [3] models, indicating that the $ANFIS_{CBO}$ model exhibits more effectiveness and accuracy. The outcomes obtained from the train, validate, and test datasets shown significant enhancements by increasing the R^2 values and decreasing the RMSE values. These outcomes may be considered when conducting a comprehensive comparison between $ANFIS_{CBO}$ and $GA - DLNN$ [3].
4. The findings of the distribution of the predicted/observed ratio indicated that $ANFIS_{CBO}$ has higher efficacy in two phases, as shown by a decrease in error variability.

Appendix

Table 3 The partial dataset

In_1	In_2	In_3	In_4	In_5	In_6	In_7	In_8	In_9	In_{10}	**Output**
400.00	4.35	8.00	1.00	2.05	3.48	2.08	15.40	13.35	7.63	1395.00
300.00	3.40	5.25	0.00	3.40	3.47	3.42	12.05	8.65	6.75	559.80
300.00	3.40	5.30	0.00	3.40	3.52	3.42	12.10	8.70	6.76	508.90
400.00	4.25	8.00	0.90	2.15	3.56	2.26	15.30	13.15	7.61	1395.00
400.00	3.40	7.30	0.00	3.40	3.49	3.39	14.10	10.70	7.28	1068.80
300.00	3.40	5.30	0.00	3.40	3.50	3.40	12.10	8.70	6.76	661.60
400.00	4.35	8.00	1.06	2.05	3.55	2.09	15.46	13.41	7.66	1321.00
400.00	3.85	7.55	0.00	2.95	3.63	3.28	14.35	11.40	7.14	1440.00
400.00	4.65	7.35	0.00	2.15	3.55	3.40	14.15	12.00	6.79	1392.00
400.00	4.35	8.00	1.06	2.05	3.56	2.10	15.46	13.41	7.66	1321.00
400.00	3.85	7.30	0.00	2.95	3.70	3.60	14.10	11.15	7.08	1440.00
300.00	3.40	5.25	0.00	3.40	3.49	3.44	12.05	8.65	6.75	559.80
300.00	3.40	5.25	0.00	3.40	3.47	3.42	12.05	8.65	6.75	585.40
400.00	3.40	7.22	0.00	3.40	3.45	3.43	14.02	10.62	7.26	1240.00
300.00	3.40	5.27	0.00	3.40	3.51	3.44	12.07	8.67	6.75	661.60
400.00	4.10	2.08	0.00	2.70	3.63	2.75	8.88	6.18	4.86	432.00
400.00	3.45	8.00	0.30	2.95	3.65	2.95	14.70	11.75	7.59	1152.00
400.00	4.75	7.40	0.00	2.05	3.55	3.35	14.20	12.15	6.76	1440.00
400.00	4.10	1.71	0.00	2.70	3.26	2.75	8.51	5.81	4.56	423.90
400.00	4.65	7.50	0.00	2.15	3.59	3.29	14.30	12.15	6.82	1551.00

Abbreviations

ML	Machine learning
GA	Genetic Algorithm
ANN	Artificial neural network
SVM	Support Vector Machine
CBO	Coot Bird Optimization
PSO	Particle Swarm Optimization
MLP	Multi-layered perceptron
WOA	Whale optimization
ANFIS	Adaptive Neuro-Fuzzy Inference System
XGB	Extreme gradient boosting
SPT	Standard penetration test
DNN	Deep neural network
CPT	Cone penetration test
R^2	Coefficient of determination
DMT	Flat dilatometer test
RMSE	Root mean square error
PMT	Pressuremeter test
NRMSE	Normalized root-mean-square
PLT	Plate loading test
RAE	Relative absolute error
DPT	Dynamic probing test
RRSE	Root relative squared error
SS	Press-in and screw-on probe test
PI	Performance index
FVT	Field vane test

Acknowledgements
I would like to take this opportunity to acknowledge that there are no individuals or organizations that require acknowledgment for their contributions to this work.

Authors' contributions
All authors contributed to the study's conception and design. Data collection, simulation, and analysis were performed by WG, J L, and S Ch. The first draft of the manuscript was written by S Ch and all authors commented on previous versions of the manuscript. All authors have read and approved the manuscript.

Funding
This research received no specific grant from any funding agency in the public, commercial, or not-for-profit sectors.

Availability of data and materials
Data can be shared upon request.

Declarations

Competing interests
The authors declare that they have no competing interests.

Received: 7 November 2023 Accepted: 12 January 2024
Published online: 12 February 2024

References

1. Sarkhani Benemaran R, Esmaeili-Falak M, Katebi H (2022) Physical and numerical modelling of pile-stabilised saturated layered slopes. Proc Inst Civ Eng Eng 175:523–538
2. Pham TA, Ly HB, Tran VQ, Van Giap L, Vu HLT, Duong HAT (2020) Prediction of pile axial bearing capacity using artificial neural network and random forest. Appl Sci 10:1871
3. Pham TA, Tran VQ, Vu HLT, Ly HB (2020) Design deep neural network architecture using a genetic algorithm for estimation of pile bearing capacity. PLoS One 15:e0243030
4. Shariatmadari N, Eslami AA, Karim PFM (2008) Bearing capacity of driven piles in sands from SPT–applied to 60 case histories
5. Esmaeili-Falak M, Katebi H, Vadiati M, Adamowski J (2019) Predicting triaxial compressive strength and Young's modulus of frozen sand using artificial intelligence methods. J Cold Reg Eng 33:4019007. https://doi.org/10.1061/(ASCE)CR.1943-5495.0000188
6. Rausche F, Goble GG, Likins GE Jr (1985) Dynamic determination of pile capacity. J Geotech Eng 111:367–383
7. Shooshpasha I, Hasanzadeh A, Taghavi A (2013) Prediction of the axial bearing capacity of piles by SPT-based and numerical design methods. Geomate J 4:560–564
8. Benali A, Nechnech A, Bouafia A (2013) Bored pile capacity by direct SPT methods applied to 40 case histories. Civ Env Res 5:118–122

9. Bouafia A, Derbala A (2002) Assessment of SPT-based method of pile bearing capacity–analysis of a database. Proc. Int. Work. Found. Des. Codes Soil Investig. View Int. Harmon. Performance-Based Des 369–74
10. Aoki N, Velloso D de A (1975) An approximate method to estimate the bearing capacity of piles. Proc., 5th Pan-American Conf. Soil Mech. Found. Eng., vol. 1, International Society of Soil Mechanics and Geotechnical Engineering Buenos …; p. 367–76.
11. Bazaraa AR, Kurkur MM (1986) N-values used to predict settlements of piles in Egypt. ASCE, Use Situ tests Geotech. Eng., pp 462–474
12. Briaud J-L, Tucker LM (1988) Measured and predicted axial response of 98 piles. J Geotech Eng 114:984–1001
13. Decourt L (1995) Prediction of load-settlement relationships for foundations on the basis of standard penetration test. Conf. cycle Intl."Zeevaert 87–102
14. Meyerhof GG (1976) Bearing capacity and settlement of pile foundations. J Geotech Eng Div 102:197–228
15. Shioi Y, Fukui J (2021) Application of N-value to design of foundations in Japan. In: Penetration Testing, volume 1. Routledge, p 159–164
16. Hoang ND, Tran XL, Huynh TC (2022) Prediction of pile bearing capacity using opposition-based differential flower pollination-optimized least squares support vector regression (ODFP-LSSVR). Adv Civ Eng 1–25. https://doi.org/10.1155/2022/7183700
17. Raja MNA, Shukla SK, Khan MUA (2022) An intelligent approach for predicting the strength of geosynthetic-reinforced subgrade soil. Int J Pavement Eng 23(10):3505–3521
18. Raja MNA, Jaffar STA, Bardhan A, Shukla SK (2023) Predicting and validating the load-settlement behavior of large-scale geosynthetic-reinforced soil abutments using hybrid intelligent modeling. J Rock Mech Geotech Eng 15:773–788
19. Raja MNA, Shukla SK (2022) An extreme learning machine model for geosynthetic-reinforced sandy soil foundations. Proc Inst Civ Eng Eng 175:383–403
20. Raja MNA, Shukla SK (2021) Multivariate adaptive regression splines model for reinforced soil foundations. Geosynth Int 28(4):368–390
21. Raja MNA, Shukla SK (2021) Predicting the settlement of geosynthetic-reinforced soil foundations using evolutionary artificial intelligence technique. Geotext Geomembranes 49:1280–1293
22. Esmaeili-Falak M, Sarkhani Benemaran R (2024) Application of optimization-based regression analysis for evaluation of frost durability of recycled aggregate concrete. Struct Concr 1–22. https://doi.org/10.1002/suco.202300566
23. Dawei Y, Bing Z, Bingbing G, Xibo G, Razzaghzadeh B (2023) Predicting the CPT-based pile set-up parameters using HHO-RF and PSO-RF hybrid models. Struct Eng Mech 86:673–686
24. Liang R, Bayrami B (2023) Estimation of frost durability of recycled aggregate concrete by hybridized Random Forests algorithms. Steel Compos Struct 49:91–107. https://doi.org/10.12989/scs.2023.49.1.091
25. Sarkhani Benemaran R, Esmaeili-Falak M, Javadi A (2022) Predicting resilient modulus of flexible pavement foundation using extreme gradient boosting based optimised models. Int J Pavement Eng 1–20. https://doi.org/10.1080/10298436.2022.2095385.
26. Esmaeili-Falak M, Benemaran RS (2023) Ensemble deep learning-based models to predict the resilient modulus of modified base materials subjected to wet-dry cycles. Geomech Eng 32(6):583–600. https://doi.org/10.12989/gae.2023.32.6.583
27. Sarkhani Benemaran R (2023) Application of extreme gradient boosting method for evaluating the properties of episodic failure of borehole breakout. Geoenergy Sci Eng 211837. https://doi.org/10.1016/j.geoen.2023.211837.
28. Aghayari Hir M, Zaheri M, Rahimzadeh N (2022) Prediction of rural travel demand by spatial regression and artificial neural network methods (Tabriz County). J Transp Res 20(4):367–386
29. Shi X, Yu X, Esmaeili-Falak M (2023) Improved arithmetic optimization algorithm and its application to carbon fiber reinforced polymer-steel bond strength estimation. Compos Struct 306:116599. https://doi.org/10.1016/j.compstruct.2022.116599
30. Zhu Y, Huang L, Zhang Z, Bayrami B (2022) Estimation of splitting tensile strength of modified recycled aggregate concrete using hybrid algorithms. Steel Compos Struct 44:389–406. https://doi.org/10.12989/scs.2022.44.3.389
31. Bui D-K, Nguyen T, Chou J-S, Nguyen-Xuan H, Ngo TD (2018) A modified firefly algorithm-artificial neural network expert system for predicting compressive and tensile strength of high-performance concrete. Constr Build Mater 180:320–333
32. Hoang N-D (2019) Estimating punching shear capacity of steel fibre reinforced concrete slabs using sequential piecewise multiple linear regression and artificial neural network. Measurement 137:58–70
33. Kurtoglu AE, Gulsan ME, Abdi HA, Kamil MA, Cevik A (2017) Fiber reinforced concrete corbels: modeling shear strength via symbolic regression. Comp and Concr 20:1–10
34. Benemaran RS, Esmaeili-Falak M (2023) Predicting the Young's modulus of frozen sand using machine learning approaches: state-of-the-art review. Geomech Eng 34:507–527
35. Hoang N-D, Tran X-L, Nguyen H (2020) Predicting ultimate bond strength of corroded reinforcement and surrounding concrete using a metaheuristic optimized least squares support vector regression model. Neural Comput Appl 32:7289–7309
36. Benemaran RS, Esmaeili-Falak M, Kordlar MS (2023) Improvement of recycled aggregate concrete using glass fiber and silica fume. Multiscale Multidiscip Model Exp Des. https://doi.org/10.1007/s41939-023-00313-2
37. Cao M-T, Nguyen N-M, Wang W-C (2022) Using an evolutionary heterogeneous ensemble of artificial neural network and multivariate adaptive regression splines to predict bearing capacity in axial piles. Eng Struct 268:114769
38. Chen W, Sarir P, Bui X-N, Nguyen H, Tahir MM, Jahed AD (2020) Neuro-genetic, neuro-imperialism and genetic programing models in predicting ultimate bearing capacity of pile. Eng Comput 36:1101–1115
39. Cheng M-Y, Cao M-T, Tsai P-K (2021) Predicting load on ground anchor using a metaheuristic optimized least squares support vector regression model: a Taiwan case study. J Comput Des Eng 8:268–282
40. Shahin MA, Jaksa MB (2005) Neural network prediction of pullout capacity of marquee ground anchors. Comput Geotech 32:153–163
41. Moradi G, Hassankhani E, Halabian AM (2022) Experimental and numerical analyses of buried box culverts in trenches using geofoam. Proc Inst Civ Eng Eng 175:311–322

42. Lee IM, Lee JH (1996) Prediction of pile bearing capacity using artificial neural networks. Comput Geotech 18:189–200. https://doi.org/10.1016/0266-352X(95)00027-8
43. Teh CI, Wong KS, Goh ATC, Jaritngam S (1997) Prediction of pile capacity using neural networks. J Comput Civ Eng 11:129–138
44. Momeni E, Nazir R, JahedArmaghani D, Maizir H (2014) Prediction of pile bearing capacity using a hybrid genetic algorithm-based ANN. Measurement 57:122–31. https://doi.org/10.1016/j.measurement.2014.08.007
45. Murlidhar BR, Sinha RK, Mohamad ET, Sonkar R, Khorami M (2020) The effects of particle swarm optimisation and genetic algorithm on ANN results in predicting pile bearing capacity. Int J Hydromechanics 3(1):69–87
46. Samui P (2011) Prediction of pile bearing capacity using support vector machine. Int J Geotech Eng 5:95–102
47. Momeni E, Armaghani DJ, Fatemi SA, Nazir R (2018) Prediction of bearing capacity of thin-walled foundation: a simulation approach. Eng Comput 34:319–327
48. Momeni E, Dowlatshahi MB, Omidinasab F, Maizir H, Armaghani DJ (2020) Gaussian process regression technique to estimate the pile bearing capacity. Arab J Sci Eng 45:8255–8267
49. Kulkarni RU, Dewaikar DM (2017) Prediction of interpreted failure loads of rock-socketed piles in Mumbai Region using hybrid artificial neural networks with genetic algorithm. Int J Eng Res 6:365–372
50. JahedArmaghani D, Shoib RSNSBR, Faizi K, Rashid ASA (2017) Developing a hybrid PSO–ANN model for estimating the ultimate bearing capacity of rock-socketed piles. Neural Comput Appl 28:391–405. https://doi.org/10.1007/s00521-015-2072-z
51. Nguyen H, Cao M-T, Tran X-L, Tran T-H, Hoang N-D (2023) A novel whale optimization algorithm optimized XGBoost regression for estimating bearing capacity of concrete piles. Neural Comput Appl 35:3825–3852. https://doi.org/10.1007/s00521-022-07896-w
52. Benesty J, Chen J, Huang Y, Cohen I (2009) Pearson correlation coefficient. Springer, Noise Reduct. speech Process., pp 1–4
53. Naruei I, Keynia F (2021) A new optimization method based on COOT bird natural life model. Expert Syst Appl 183:115352
54. Mokhtarzad M, Eskandari F, Jamshidi Vanjani N, Arabasadi A (2017) Drought forecasting by ANN, ANFIS, and SVM and comparison of the models. Environ Earth Sci 76:1–10
55. Rumelhart DE, Hinton GE, McClelland JL (1986) A general framework for parallel distributed processing. Parallel Distrib Process Explor Microstruct Cogn 1:26
56. Anderson JA (1995) An introduction to neural networks. MIT Press, Massachusetts
57. Coulibaly P, Anctil F, Bobée B (2000) Daily reservoir inflow forecasting using artificial neural networks with stopped training approach. J Hydrol 230:244–257
58. Maiti S, Tiwari RK (2014) A comparative study of artificial neural networks, Bayesian neural networks and adaptive neuro-fuzzy inference system in groundwater level prediction. Environ Earth Sci 71:3147–3160
59. Jang J-S (1993) ANFIS: adaptive-network-based fuzzy inference system. IEEE Trans Syst Man Cybern 23:665–685
60. Kisi O, Demir V, Kim S (2017) Estimation of long-term monthly temperatures by three different adaptive neuro-fuzzy approaches using geographical inputs. J Irrig Drain Eng 143:4017052
61. Azad A, Farzin S, Kashi H, Sanikhani H, Karami H, Kisi O (2018) Prediction of river flow using hybrid neuro-fuzzy models. Arab J Geosci 11:1–14
62. Khatti J, Grover KS (2023) Prediction of compaction parameters of soil using GA and PSO optimized relevance vector machine (RVM). ICTACT J Soft Comput 13(2):2890–2903. https://doi.org/10.21917/ijsc.2023.0409

Publisher's Note